ENERGY DISSIPATING STRUCTURES: A STRUCTURES - MATERIALS - DESIGN SYNTHESIS

GEORGE GERARD

TECHNICAL REPORT No. 268-1

11 AUGUST 1964

prepared for
CONTRACT NO. NASw-928
NATIONAL AERONAUTICS AND SPACE ADMINISTRATION
WASHINGTON 25, D. C.

ALLIED RESEARCH ASSOCIATES, INC.
VIRGINIA ROAD • CONCORD, MASSACHUSETTS

SUMMARY

An analysis of several forms of ideal energy dissipating mechanisms is presented which synthesizes the weight or mass index in terms of pertinent design indices, structural efficiency and material efficiency parameters. For the landing problem, the primary design index is the touchdown velocity while a secondary design index is associated with the payload fragility in terms of deceleration and onset rate limitations.

The structural design of energy dissipators is then considered in terms of structural and material efficiency parameters. It is shown that the large body of available information on optimum structural design is directly applicable to energy dissipators and has an important bearing on attainable structural efficiencies. Finally, various forms of cylindrical shell dissipators such as buckled and frangible tubes and pressurized membranes and shells are compared to establish their relative efficiencies.

LIST OF SYMBOLS

A	area, in^2
C	buckling coefficient
D	design index
E	elastic modulus, psi
E_{sub}	energy
g	planetary gravitational constant, ft/sec^2
g_a	payload deceleration fragility, ft/sec^2
$\dot{g}_a$	payload onset fragility, ft/sec^3
L	length of dissipator, in
m	mass
M	material efficiency
n	number of dissipators
P	load, lb
R	radius
s	stroke, ft
S	structural efficiency
t	time or thickness
V_i	touchdown velocity, ft/sec or in/sec
w	weight, lb
W	weight index
λ	design index, $\lambda = g_a^2/V_i\dot{g}_a$
ρ	density, psi
σ	stress, psi
$\bar{\sigma}$	axial compressive stress, psi
σ_{cy}	compressive yield strength, psi
σ_o	optimum stress, psi

Subscripts

c	combined dissipator
d	deceleration limiter
o	onset limiter
v	vehicle

TABLE OF CONTENTS

ENERGY DISSIPATING STRUCTURES: A STRUCTURES - MATERIALS - DESIGN SYNTHESIS

1. INTRODUCTION

The need of a soft landing capability for spacecraft alighting on earth, lunar or other planetary surfaces has focussed considerable attention on various forms of energy dissipation systems. Inherent in the design of such systems for space applications are stringent requirements on weight, reliability and storability, all in the presence of a space environment. It is to be noted that Esgar has presented a comprehensive review of this field in Ref. 1.

The basic performance requirements of an energy dissipation system can be prescribed in terms of the payload fragility: allowable onset rate and peak deceleration. Hence, the essential feature of the energy dissipator is the control of the spacecraft landing behavior compatible with the prescribed payload fragility parameters.

Because of the various types of energy dissipation systems that have been proposed and can be contemplated, there exists a need to compare such systems on a common basis so that their relative efficiency can be established in terms of specified performance requirements. As a consequence, this study is concerned with the establishment of suitable structural and material efficiency parameters and design indices for idealized energy dissipators. The results are obtained in sufficiently general form that they may be applicable to various systems provided that they conform to the ideal system used in the analysis.

In order to establish general conclusions concerning the relative efficiencies of various types of energy dissipators, it is necessary to introduce various assumptions which limit the scope of this study. As a consequence, this investigation is concerned not with the overall landing system comprising landing struts and energy dissipators, but solely with the energy dissipator itself.

Furthermore, the deceleration characteristics of a vehicle employing an ideal energy dissipator are assumed to be those in Fig. 1. As indicated, the vehicle would experience a linear increase in deceleration at a constant deceleration until the vehicle has been brought to rest. With the deceleration-time signature shown in Fig. 1, the landing system arrests vehicle motion consistent with the maximum loads which can be tolerated by the payload. Hence, the associated weight and stroke of the landing system should be a minimum.

It is convenient to consider the ideal energy absorber to be composed of an onset limiter and deceleration limiter with the associated regions of operation indicated in Fig. 1. In this manner, the characteristics of each element of the system can be studied separately, and the analysis of the composite system follows from the integration of its elements.

FIG. 1

VEHICLE DECELERATION TIME HISTORY FOR AN IDEAL ENERGY DISSIPATOR

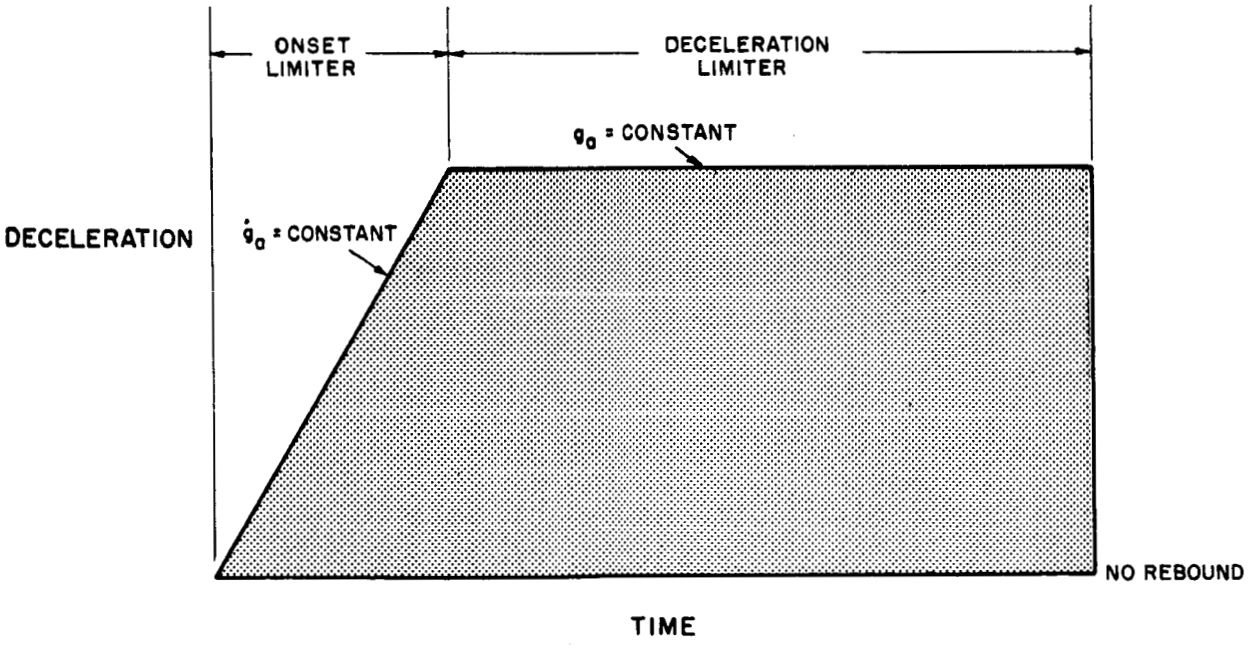

2. DESIGN SYNTHESIS

Deceleration Limiter

In order to establish some preliminary results concerning the parameters of importance for energy dissipators as may be used in spacecraft landing systems, we shall consider first a particularly simple form of ideal energy dissipator, the deceleration limiter. As shown in Fig. 2a, the deceleration limiter is characterized by a rectangular shape with an infinite onset rate, a horizontal allowable payload deceleration of g_a and a stroke, s. The payload fragility is given by g_a and is presumably established by tests conducted on earth. Considerations of onset rate limitations are reserved for a later section.

Regardless of the type of energy dissipator that may be utilized, the energy to be dissipated is that associated with the spacecraft. It is assumed that the vehicle touchdown kinetic energy is much greater than the vehicle potential energy change associated with the stroke of the energy dissipator. Consequently, the energy to be dissipated is simply

$$E_v = (1/2)\, m_v V_i^2 \tag{1}$$

Returning to Fig. 2a, the energy dissipation associated with the total number of deceleration limiters used on the spacecraft is given by

$$E_d = g_a m_v s_d \tag{2}$$

By equating Eqs. (1) and (2), we can establish a result concerning the stroke, s, which relates the prescribed touchdown velocity and deceleration limit, g_a,

$$s_d = V_i^2/2g_a \tag{3}$$

For the deceleration limiter, the decelerating force is constant and if the dissipator operates at a constant average stress level, $\bar{\sigma}$, then

$$g_a m_v = \bar{\sigma} A_d \tag{4}$$

By substituting Eq. (4) into (2)

$$E_d = \bar{\sigma} A_d s_d \tag{5}$$

FIG. 2

IDEAL ENERGY DISSIPATORS

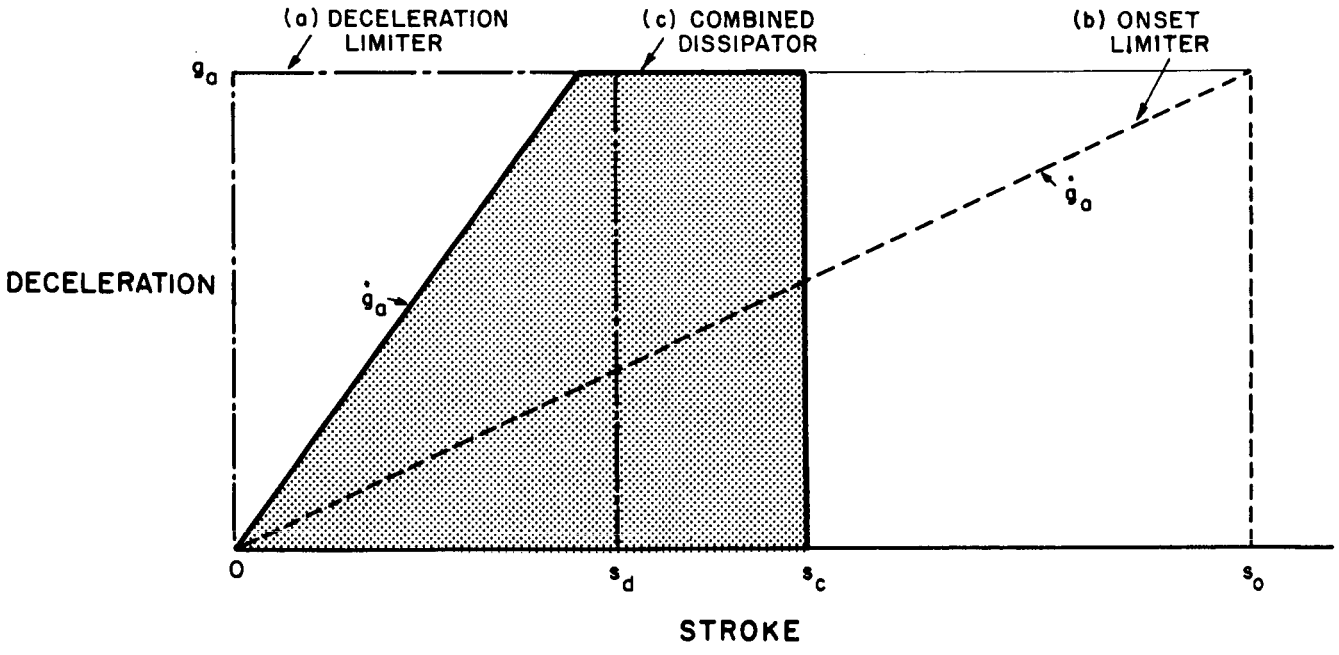

The mass of the dissipator is simply

$$m_d = (\rho/g)A_d L \tag{6}$$

In Eq. (6), it is to be noted that L represents the length of the dissipator which is usually greater than the stroke, s_d. This difference is associated with the "crushability" of the dissipator material and can have an important effect on efficiency.

By eliminating A_d in Eqs. (5) and (6) and equating the energies associated with Eqs. (1) and (5), the following relationship is obtained:

$$m_d/m_v = (1/2)\,(L/s_d)\,(\rho/g\bar{\sigma})\,V_i^2 \tag{7}$$

This equation represents the design synthesis for the ideal deceleration limiter and can be represented in the following form which is general for design synthesis investigations:

$$W = S \cdot M \cdot D \tag{8}$$

where:

W = weight or mass index $(=m_d/m_v)$

S = structural efficiency $(=L/s_d)$

M = material efficiency $(=\rho/g\bar{\sigma})$

D = design index $(=V_i^2)$

It is to be noted that if the energy dissipator operates through some buckling mechanism, then $\bar{\sigma}$ depends strongly upon the structural configuration of the dissipator. In this case the S and M efficiencies are interrelated.

Preliminary Results

At this point, it is of interest to obtain some preliminary results from the design synthesis of the ideal deceleration limiter. For this purpose Fig. 3 has been prepared using Eq. (7). The values chosen for $\bar{\sigma}/\rho$ are shown on the sloping lines of Fig. 3 together with values of the corresponding parameter E_d/w (ft-lb/lb) currently used to represent the efficiency of the energy absorbing material. For the units shown in Fig. 3, the two efficiency parameters are related simply by

$$E_d/w = \bar{\sigma}/12\rho \tag{9}$$

FIG. 3

DESIGN SYNTHESIS FOR DECELERATION LIMITERS OF 2024 - T3 ALUMINUM ALLOY, $s_d/L = 0.8$

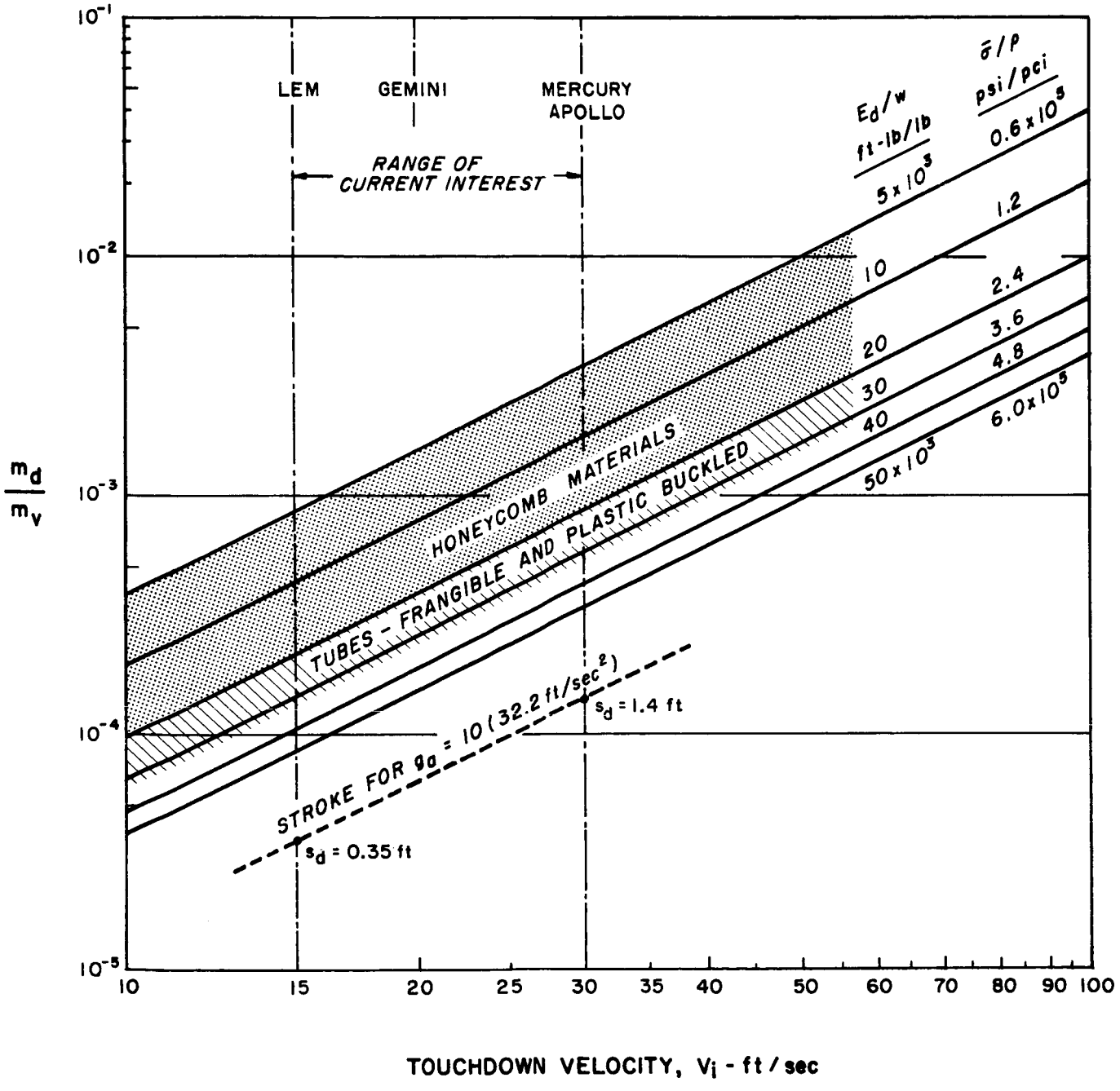

Also shown in Fig. 3 are some representative ranges of currently available dissipators of 2024-T3 aluminum alloys such as honeycomb materials and both frangible and plastic buckled tubes. For these dissipators, a value of $s_d/L = 0.8$ has been assumed as a representative value.

The range of current interest for spacecraft touchdown velocities is indicated in Fig. 3. It can be observed that the energy dissipator weights can indeed be a small fraction of that of the vehicle particularly as $\bar{\sigma}/\rho$ is increased. For reference purposes, the stroke requirement based up on Eq. (3) for a maximum deceleration of $g_a = 10g$ is shown in the lower portion of Fig. 3. It can be observed that reasonable strokes are obtained within the touchdown velocity range of current interest.

The preliminary results which have been established are based upon the ideal deceleration limiter and hence neglect the influence of onset rate limitations imposed by the payload fragility. As a consequence, it is the objective now to first analyze the ideal onset rate limiter shown in Figure 2b and then consider the more realistic model of an ideal combined onset and deceleration limiter shown in Figs. 1 and 2c. From this study, the influence of onset rate limitations upon the design synthesis can be evaluated.

Onset Limiter

The distinguishing feature of the ideal onset limiter shown in Fig. 2b is that the onset rate is given by $\dot{g}_a$ = constant and thus the force generated by the energy dissipator and resisting vehicle motion increases linearly with time. As indicated in Ref. 2, it is possible in a practical sense to shape honeycomb materials in a manner corresponding closely to the ideal onset limiter. It also appears feasible to utilize a similar shaping technique for other types of structural materials and energy dissipators.

For a given touchdown velocity, V_i, and onset deceleration rate, $\dot{g}_a$, the following stroke relationship characterizes the ideal onset limiter (Ref. 3)

$$s_o = V_i t - \dot{g}_a t^3/6 \tag{10}$$

The time required for the dissipator to reach zero velocity and thus absorb all of the input energy is obtained by equating the derivative of Eq. (10) to zero. Thus,

$$t = (2V_i/\dot{g}_a)^{\frac{1}{2}} \tag{11}$$

By substituting Eq. (11) into (10), the following relation between stroke and the prescribed touchdown velocity and onset rate is obtained.

$$s_o = (2V_i)^{\frac{1}{2}}/3(\dot{g}_a)^{\frac{1}{2}} \tag{12}$$

Since deceleration is linear with time, the deceleration at the end of the stroke is simply

$$g_a = \dot{g}_a t \tag{13}$$

By use of Eqs. (11), (12) and (13), the following relation among stroke, touchdown velocity and allowable deceleration is obtained.

$$s_o = (4/3)(V_i^2/g_a) \tag{14}$$

At this point, it is interesting to compare the relative strokes of the onset and deceleration limiters for prescribed values of V_i^2/g_a. From Eqs. (14) and (3),

$$s_o/s_d = 8/3 \tag{15}$$

Thus, for the same energy dissipation, the stroke of the onset limiter is significantly larger. This is obviously the disadvantage in using the onset limiter alone as the energy dissipator.

From the analysis presented in Ref. 3 for the onset limiter which parallels that given herein for the deceleration limiter, the design synthesis relation for the onset limiter operating at a constant stress level, $\bar{\sigma}$, is given by

$$m_o/m_v = (1/6)[4(L/s_o)^2-1](\rho/g\bar{\sigma})V_i^2 \tag{16}$$

It is to be noted from Eq. (16) as compared to Eq. (7) for the deceleration limiter that for $s/L = 1$, the mass ratios are identical and only the strokes differ significantly. For $s/L < 1$,

$$m_o/m_d = (1/3)(s_d/L)[4(L/s_o)^2-1] \tag{17}$$

It is apparent from Eq. (17) that the mass of an onset limiter will always be greater than that of the deceleration limiter for the same value of s/L.

Combined Energy Dissipator

Although the onset limiter does not compare particularly favorably with the deceleration limit, it is obvious that payload fragility considerations require the use of an onset limiter in combination with a deceleration limiter. This combined energy dissipator is shown in an ideal form in Figs. 1 and 2c, and the total stroke is simply

$$s_c = s_o + s_{dc} \tag{18}$$

From Eqs. (10) and (13)

$$s_o = \lambda(1-\lambda/6)\,(V_i^2/g_a) \tag{19}$$

where: $\lambda = g_a^2/V_i\dot{g}_a$

Note that λ is a nondimensional parameter that combines the three performance requirements for the energy dissipator into a convenient design index. By comparing Eqs. (19) and (14), it can be observed that $\lambda = 2$ for the simple onset limiter.

For the deceleration limiter phase, the stroke requirement is given by Eq. (3) based on the velocity at the end of the onset limiter stroke, V_d, rather than V_i

$$V_d = V_i - g_a^2/2\dot{g}_a \tag{20}$$

By combining Eqs. (3) and (2a) in the manner indicated

$$s_{dc} = (1/2)\,(1-\lambda+\lambda^2/4)\,(V_i^2/g_a) \tag{21}$$

From the definition of λ given in Eq. (19), it can be observed that $\lambda = 0$ characterizes the simple deceleration limiter since $\dot{g}_a = \infty$.

The total stroke for the combined energy dissipator as compared to that for the simple deceleration limiter is obtained by suitable combining Eqs. (19), (21) and (3). Thus,

$$s_o/s_d = 1+\lambda-\lambda^2/12 \tag{22}$$

For $0 \leq \lambda \leq 2$; $1 \leq (s_o/s_d) \leq (8/3)$ which represents the range of values between the simple deceleration and onset limiters, respectively.

From the analysis presented in Ref. 3 for the combined energy dissipator, the following mass ratio can be established between the combined dissipator and the simple deceleration limiter for the case where the $\bar{\sigma}/\rho$ and s/L values are the same for the onset and deceleration phase.

$$m_c/m_d = 1+\lambda \left(\frac{L^2}{s_c} - 1\right) - \frac{\lambda^2}{12}\left(2\,\frac{L}{s_c} - 3 + \frac{s_c}{L}\right) \qquad (23)$$

By combining Eqs. (23) and (7), the following design synthesis relationship is obtained for the combined energy dissipator

$$m_c/m_v = (1/2)\,(L/s_c)\,(m_c/m_d)\,(\rho/g\bar{\sigma})\,V_i^2 \qquad (24)$$

Here, as compared to the simple deceleration limiter, the structural efficiency of the combined dissipator depends upon the design index λ as well as s/L. In all other respects the situation is the same as for the decleration limiter.

In Fig. 4, numerical results are presented for the stroke ratio represented by Eq. (22) and the mass ratio represented by Eq. (23) as a function of the design index, λ. For the mass ratio, s_c/L values of 1.0 and 0.8 were used for the calculations.

Design Synthesis Results

By use of Eq. (24) in conjunction with Fig. 4, the results presented in the design synthesis chart of Fig. 5 were obtained. In this case, as compared to Fig. 3, the influence of the material efficiency parameter $g\bar{\sigma}/\rho$ is suppressed in order to assess the effect of λ and s_c/L on the structural efficiency of the combined energy dissipator. For this purpose, values of $s_c/L = 1.0$ and 0.8 were used together with the entire $0 \leq \lambda \leq 2$ range.

Examination of Fig. 5 reveals that the most important variable is the design index V_i. It has already become apparent from Fig. 3 that the material efficiency parameter $\bar{\sigma}/\rho$ is of major significance. From the results shown in Fig. 5, s_c/L has some second order effect on the structural efficiency whereas the design index λ plays some role only for $s_c/L < 1.0$.

Within the touchdown velocity range of current interest for the spacecraft shown in Fig. 5, representative values of λ are generally considerably less than 0.5. As a consequence we can conclude that the offset deceleration requirement as represented by the design index, λ, plays a minor role for spacecraft of current interest as far as the mass ratio is concerned. Thus, for preliminary evaluation purposes,

the design synthesis based on the deceleration limiter can be utilized to evaluate the first order (V_i, $\bar{\sigma}/\rho$) and second order (s_c/L) effects. When considering stroke requirements, consideration of λ may be necessary.

FIG. 4

STROKE AND MASS RATIOS FOR COMBINED ENERGY DISSIPATOR COMPARED TO SIMPLE DECELERATION LIMITER

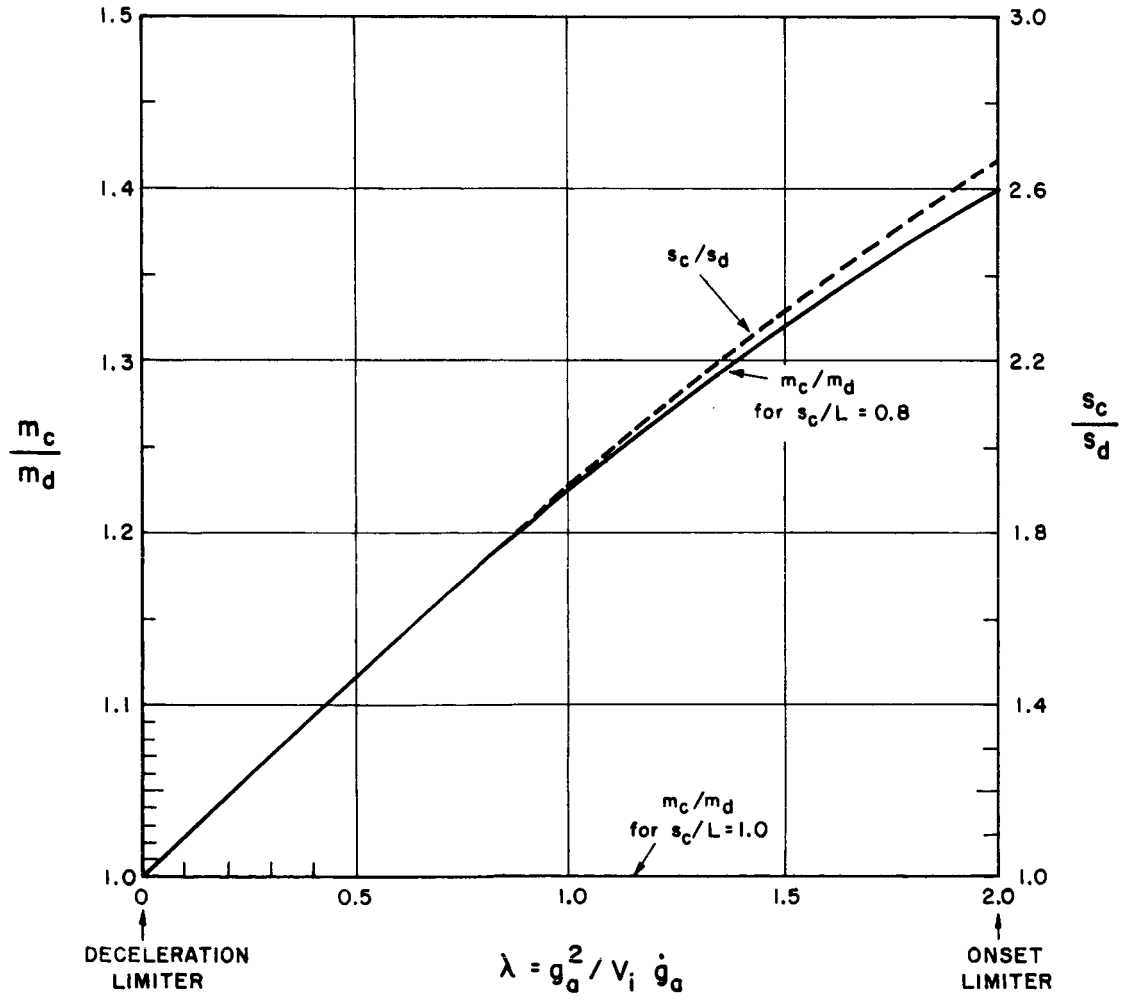

FIG. 5

DESIGN SYNTHESIS FOR COMBINED ENERGY DISSIPATORS

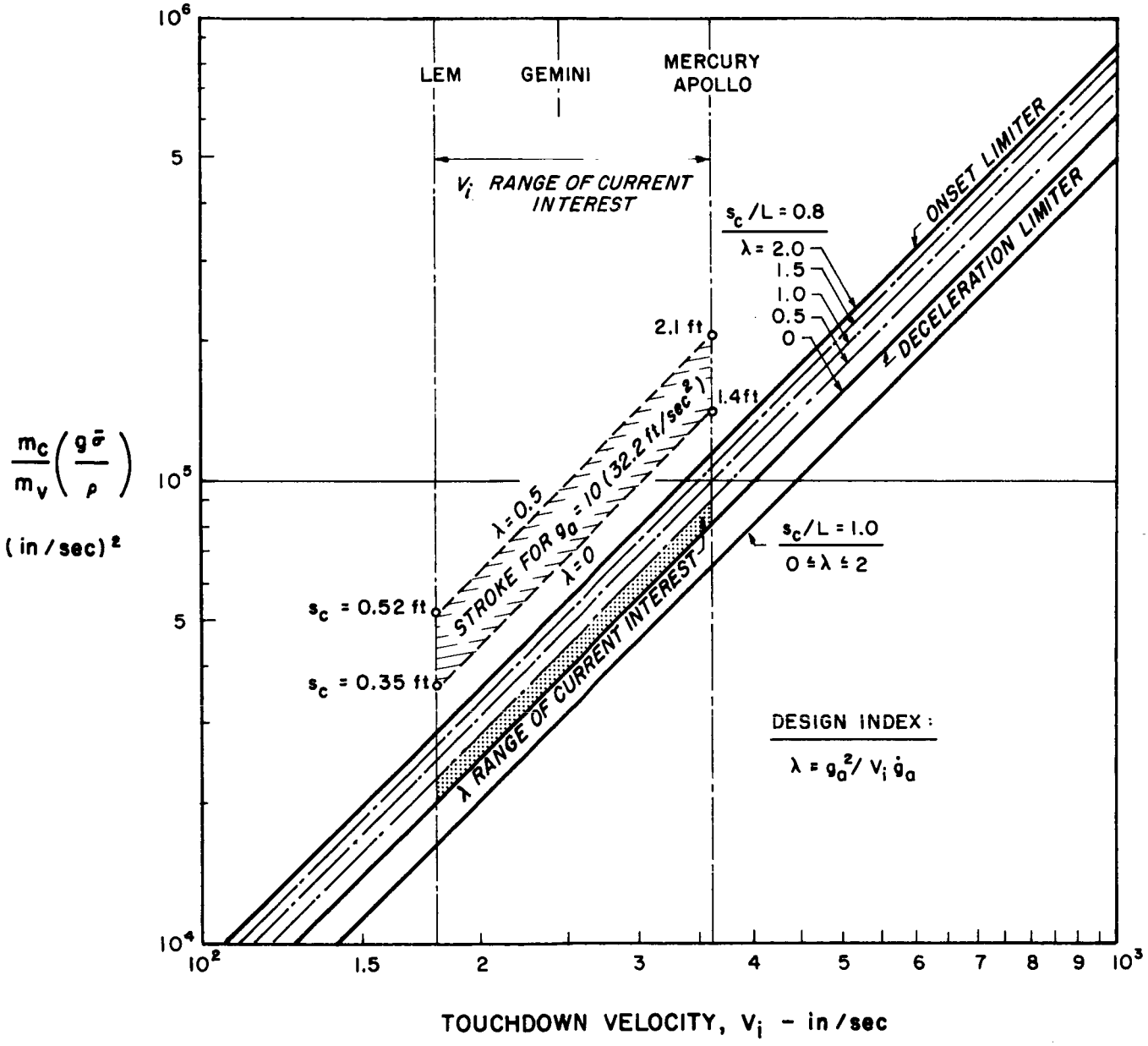

3. STRUCTURAL DESIGN OF ENERGY DISSIPATORS

The analysis and results presented in Section 2 are concerned with the generalized performance of ideal energy dissipators. From Eqs. (23), (24) and the results presented in Fig. 5, it is apparent that the efficiency of the dissipators depend significantly upon $\bar{\sigma}$ and to a lesser extent upon s_c/L for prescribed values of the design indices V_i and λ.

It is pertinent now to focus attention upon $\bar{\sigma}$ in order to evaluate the relative efficiencies of various types of energy dissipating structures. Since many of the dissipators operate under compressive loading and are consequently subject to buckling considerations, $\bar{\sigma}$ can depend strongly upon the structural configuration of the dissipator as well as the mechanical properties of the materials utilized.

The Design Problem

In considering $\bar{\sigma}$, it is to be noted that the energy dissipated depends solely upon the average constant stress $\bar{\sigma}$ developed in the direction of the stroke. Hence, the design problem for energy dissipators can be specified in terms of a load carrying requirement and a stroke requirement for prescribed values of the vehicle performance parameters.

The load carrying requirement per dissipator is

$$P = g_a m_v / n \tag{25}$$

The stroke required for energy dissipation from Eqs. (22) and (3)

$$s_c = (1/2)(1 + \lambda - \lambda^2/12) V_i^2 / g_a \tag{26}$$

Since the load and stroke are prescribed in terms of the vehicle performance parameters, these two quantities can be conveniently combined in terms of the following loading index which is a fundamental design parameter in minimum weight analyses of structures subjected to buckling (Ref. 4).

$$P/L^2 = (P/s_c^2)(s_c/L)^2 \tag{27}$$

By substituting Eq. (26) into (27)

$$P/L^2 = \frac{4\, g_a^3\, m_v (s_c/L)^2}{n\, V_i^4 (1 + \lambda - \lambda^2/12)^2} \tag{28}$$

It can be observed from Eq. (28) that the loading index P/L^2 can be varied somewhat only through n, the number of energy dissipators utilized. All other quantities are specified except for s_c/L which has a small influence on P/L^2.

Eq. (28) essentially establishes a relation between the design synthesis of energy dissipators and the large body of available information on minimum weight analysis. Hence, Eq. (28) represents a rather important result for establishing the optimum value of $\bar{\sigma}$ for various forms of energy dissipators.

Optimum Design

Because of its importance in several types of energy dissipators, it is pertinent to consider the minimum weight design of a thin wall circular tube which buckles simultaneously as a pin-ended column and in the local instability mode. It is assumed here that energy dissipation occurs by collapse of the tube in the local instability mode and that column failure does not occur. Thus the optimum design based on simultaneous buckling of the two instability modes provides a lower bound for the energy dissipator.

Following the development in Ref. 4, the column stress for a thin wall pin-ended circular tube is given by

$$\sigma_{co} = (\pi^2/2)\, E\, (R/L)^2 \tag{29}$$

The local buckling stress of the thin walls is

$$\sigma_{cr} = C\, E\, (t/R) \tag{30}$$

The applied stress

$$\sigma_a = P/2\pi Rt \tag{31}$$

By combining Eqs. (29) to (31) in the following form and letting $\sigma_{co} = \sigma_{cr} = \sigma_a = \sigma_o$, the optimum stress for minimum weight is obtained

$$\sigma_o = (\sigma_{co}\, \sigma_{cr}\, \sigma_a)^{\frac{1}{3}} = [(\pi C/4)\, P\, E^2/L^2]^{\frac{1}{3}} \tag{32}$$

In order to have the results in a nondimensional form for illustrative purposes, Eq. (32) can be divided by the compressive yield strength, σ_{cy} with the following result

$$\sigma_o/\sigma_{cy} = (\pi C/4)^{\frac{1}{3}} \; (E/\sigma_{cy}) \; (P/EL^2)^{\frac{1}{3}} \qquad (33)$$

Numerical results obtained by use of Eq. (33) are shown in Fig. 6 for several values of E/σ_{cy} and C = 0.25 which is typical of test data on local buckling of cylinders. A horizontal cut-off at $\sigma_o/\sigma_{cy} = 1$ has been assumed which corresponds to an idealized stress-strain curve.

It can be observed from Fig. 6 that depending upon the value of the loading index, P/L^2, stability limitations require an optimum stress for minimum weight less than the compressive yield strength. The primary feature of the results in Fig. 6 is that use of stress level other than σ_o for a given P/L^2 results in a design of higher weight than the minimum associated with σ_o.

Thus, the data shown in Fig. 3, for example, which represent the maximum attainable energy dissipation in terms of $\overline{\sigma}/\rho$, may not be necessarily the most efficient values from a minimum weight standpoint when the optimum design problem is considered. It is the design conditions represented by P/L^2 and the material properties represented by σ_{cy}, E and ρ which determine the appropriate strength-weight ratio, σ_o/ρ, for minimum weight of the energy dissipator rather than the maximum values attainable. Only when the P/L^2 values fall in the strength region shown in Fig. 6 can the latter be utilized.

Although the P/EL^2 range of current interest for soft landing of spacecraft remains to be established, preliminary indications are that the 10^{-7} to 10^{-6} range may be representative. From Fig. 6, it is evident that because of stability limitations within this region there is no advantage is using high strength materials as represented by $E/\sigma_{cy} = 100$. Lower strength materials such as $E/\sigma_{cy} = 200$ or higher should be completely adequate in this region. Thus, it can be observed that the optimum design results are useful in establishing conclusions on material efficiency as well as structural efficiency.

Cylindrical Shell Energy Dissipators

In order to relate the optimum design results on tubes to various forms of cylindrical shell energy dissipators such as buckled tubes, it is pertinent to consider their relative efficiencies in terms of stress. In this manner, the inherent maximum efficiencies of such devices can be assessed. Practical considerations involved in the design and utilization of energy dissipator systems in spacecraft may, of course, modify to some extent conclusions based solely upon optimum stress considerations.

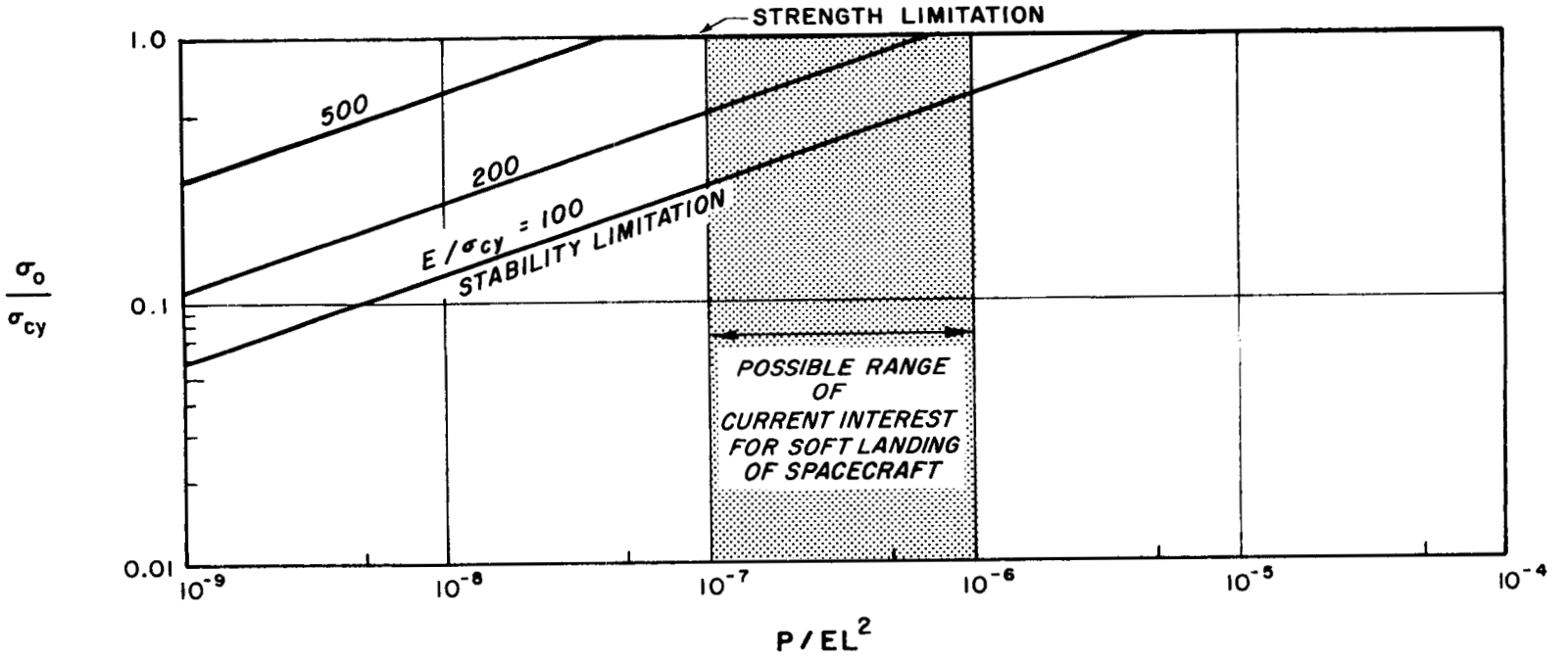

FIG.6

OPTIMUM DESIGN OF CIRCULAR TUBES UNDER COMPRESSION

The buckled tube as an energy dissipator has been considered in the optimum design example and the results presented in Fig. 6 are representative of the maximum efficiency that can be realized. Because of column stability limitations associated with the stroke requirements, the optimum stress level is limited. For the possible P/EL^2 range of current interest indicated in Figs. 6 and 7, moderate strength materials characterized by $E/\sigma_{cy} = 200$ or greater can be utilized since there is no advantage in using those of higher strength within this P/EL^2 range.

Turning now to the frangible tube (Ref. 5) which dissipates energy through fragmentation of a thin wall circular tube expanding over a die, we find that the same stability considerations inherent in the buckled tube govern the structural design of the frangible tube in spacecraft applications. Since the frangible tube is in compression and must not buckle in either the column or local instability modes, the fragmentation stress in the stroke direction must always be less than the optimum stress for the buckled tube. Thus, the results presented in Figs. 6 and 7 represent an upper bound for the efficiency of frangible tube energy dissipators. The same efficiency considerations apply, therefore, to both the frangible and buckled tubes.

The gas bag as an energy dissipator (Ref. 1) can be represented as a cylindrical membrane prestressed by internal pressure. Thus, the axial tensile stress in the membrane is one-half of that in the circumferential direction which can be taken as the yield strength for our purposes here. Since the axial compressive load carrying ability of the cylindrical membrane is equal to the axial tensile prestress (Ref. 7)

$$\overline{\sigma} = (1/2)\sigma_y \tag{34}$$

Thus, for materials of the same strength level, the gas bag (neglecting the weight of the gas and end closure membranes) is potentially only half as efficient as the buckled and frangible tubes as shown in Fig. 7 at the higher values of P/EL^2. At the lower values of P/EL^2 where stability considerations limit the buckled and frangible tubes, the gas bag can be more efficient for materials of the same strength level.

Coppa in Ref. 6 proposed the use of a pressurized shell as an energy dissipator. This device utilizes the tension prestress of pressurization and the compressive load carrying ability associated with buckling and thus increases the axial load carrying ability as compared to the gas bag or buckled tube. Since the

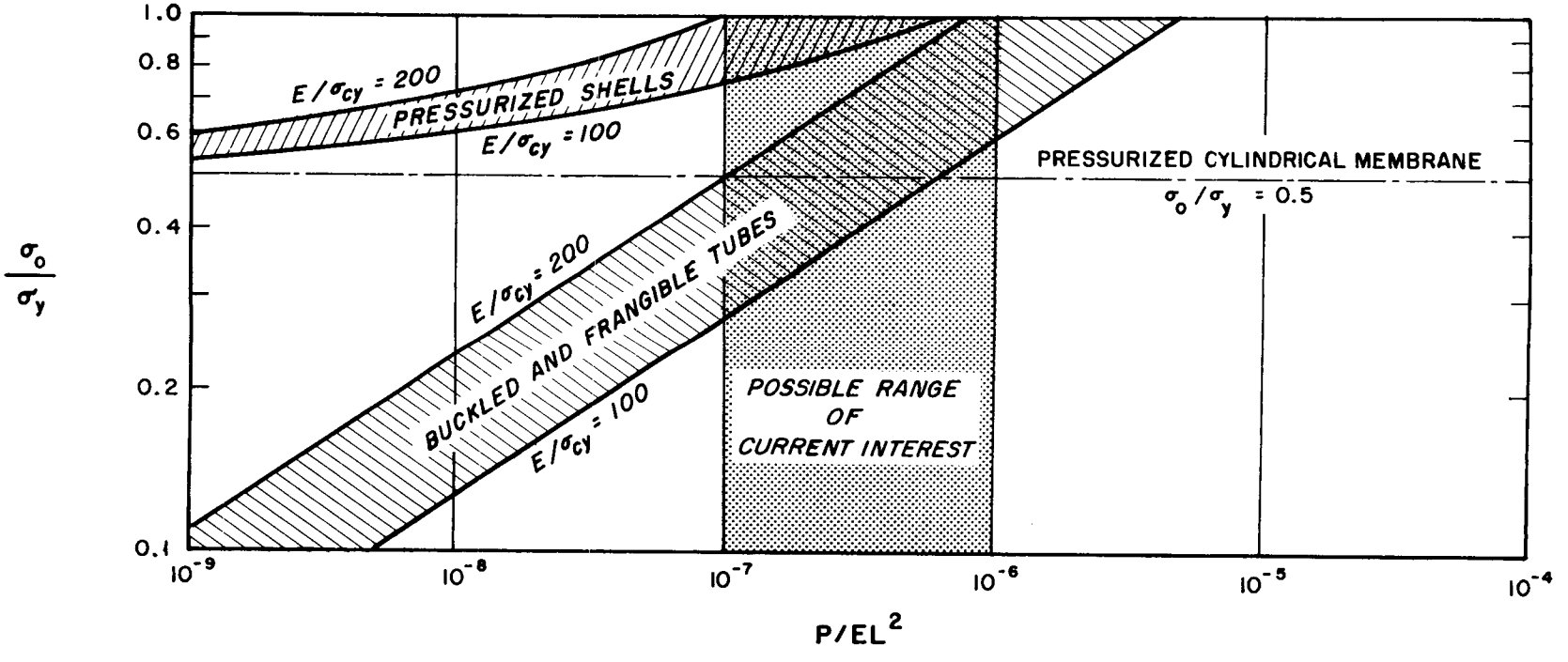

FIG. 7

COMPARATIVE EFFICIENCIES OF SEVERAL TYPES OF CYLINDRICAL SHELL ENERGY DISSIPATORS

pressurized shell is in compression, it is subject to the same stability considerations as the buckled tube and therefore the associated axial compressive stress (Ref. 7)

$$\overline{\sigma} = (\sigma_y/2) + \sigma_o \tag{35}$$

The first term in Eq. (35) represents the tension prestress and the second the compressive buckling contribution associated with the optimum stress of Fig. 6.

As shown in Fig. 7, the pressurized shell (neglecting the weight of the gas and end closures) can potentially increase the efficiency of the buckled tube in a limited range and is inherently more efficient than the gas bag.

While the results presented in Figs. 6 and 7 are in terms of stress, it is also possible to present the design synthesis results directly in terms of the mass ratio and toucndown velocity in the form of Fig. 4. By substituting Eq. (32) and (24) and noting that the P/L^2 values are given by Eq. (28) for specified design conditions, we obtain

$$\frac{m_c}{m_v}\left(\frac{m_d}{m_c}\right)\frac{s_c}{L} = \frac{1}{2}\left(\frac{\rho}{gE}\right)\left(\frac{4}{\pi C}\right)^{\frac{1}{3}}\left(\frac{EL^2}{P}\right)^{\frac{1}{3}} V_i^2 \tag{36}$$

Numerical results based on Eq. (36) are presented in Fig. 8 using a value of $gE/\rho = 3.86 \times 10^8$ $(in/sec)^2$ which is representative of many materials at room temperature. Also shown in Fig. 8 is the range of possible interest of V_i and P/EL^2 for current spacecraft. The presentation of Fig. 8 combines the energy dissipator design synthesis and optimum design results in a particularly useful form.

FIG. 8

DESIGN SYNTHESIS BASED UPON OPTIMUM DESIGN OF BUCKLED TUBES

$gE/\rho = 3.86 \times 10^8 \text{ (in/sec)}^2$

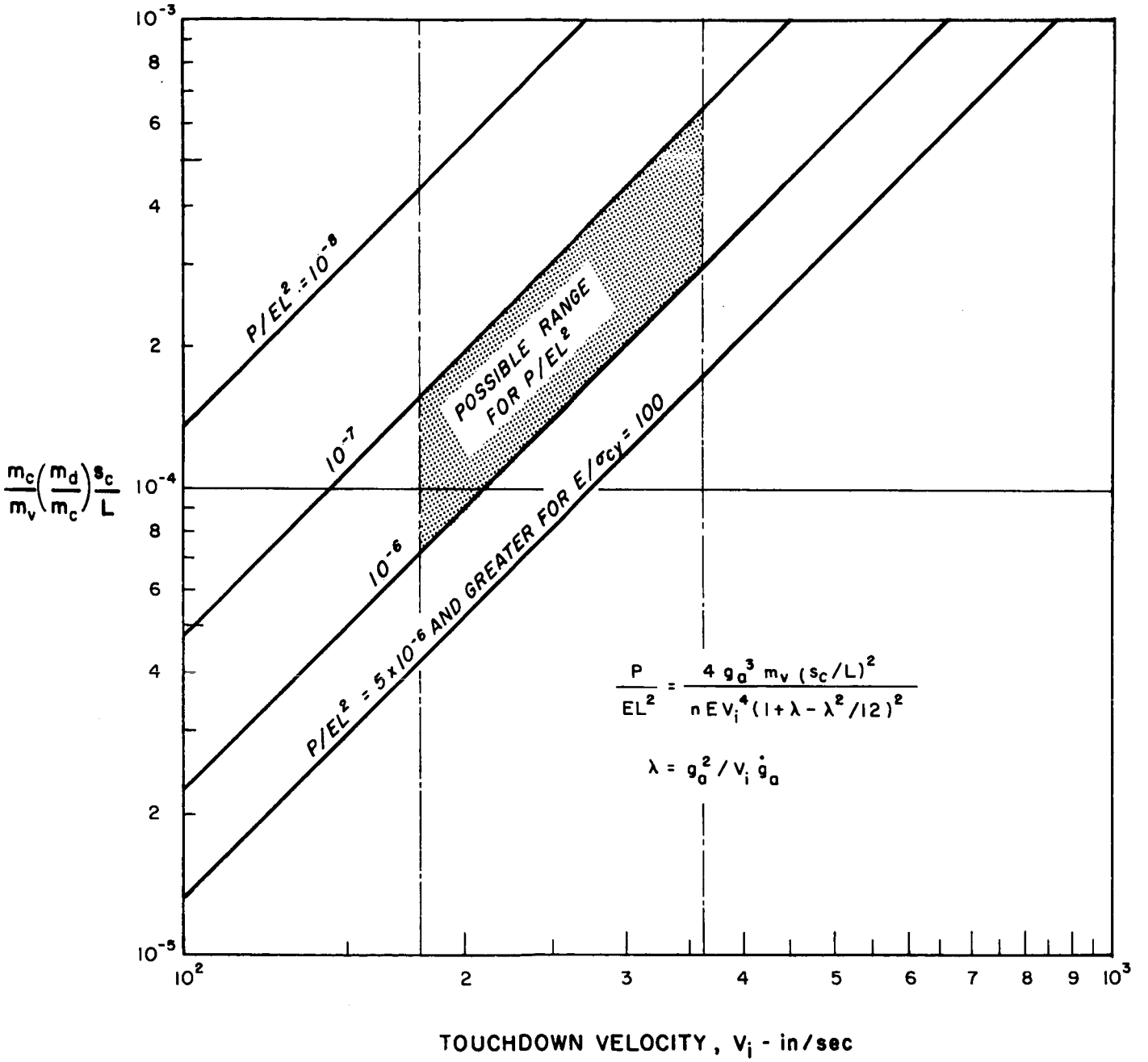

REFERENCES

1. Esgar, J.B.,"Survey of Energy-Absorption Devices for Soft Landing of Space Vehicles," NASA TN D-1308, June 1962.

2. Brooks, G.W. and H.D. Carden, "A Versatile Drop Test Procedure for the Stimulation of Impact Environments," Noise Control Shock and Vibration, Vol. 7, No. 5, pp. 4-8, Sept.–Oct. 1961.

3. Milligan, R. and G. Gerard, "Weight and Performance Design Indices for Idealized Spacecraft Landing Systems," NASA CR 53320, (Allied Research Associates Tech. Rept. 235-6), March 1964.

4. Gerard, G., Minimum Weight Analysis of Compression Structures, New York University Press, New York, 1956.

5. McGehee, J.R., "A Preliminary Experimental Investigation of an Energy-Absorption Process Employing Frangible Metal Tubing," NASA TN D-1477, October 1962.

6. Coppa, A.P., "Collapsible Shell Structures for Lunar Landings," American Rocket Society Preprint 2156-61, October 1961.

7. Williams, M.L., G. Gerard and G.A. Hoffman, "Selected Areas of Structural Research in Rocket Vehicles," XI International Astronautical Congress, Stockholm, Vol. 1, pp. 146-166, 1960.